Continuous-Wave Nd:YVO$_4$ self-Raman lasers operating at 1109nm, 1158nm and 1231nm

Ran Li,[*] **Ralf Bauer, and Walter Lubeigt**

Centre for Microsystems and Photonics, Department of Electronic and Electrical Engineering, University of Strathclyde, Glasgow, G1 1XW, UK
[*]ran.li@strath.ac.uk

Abstract: Several continuous-wave Nd:YVO$_4$ self-Raman lasers based on the primary and secondary Raman transitions of YVO$_4$ (893cm^{-1} and 379cm^{-1} respectively) are reported in this paper. Laser outputs were obtained at a wavelength of 1109nm, 1158nm and 1231nm with maximum output powers of 1.0W, 700mW and 540mW respectively. The respective absorbed pump power to Raman output power conversion efficiencies were measured at 8.4%, 5.4%, and 5.4%.

References and links

1. P. Cerny, H. Jelinkova, P. G. Zverev, and T. T. Basiev, "Solid state lasers with Raman frequency conversion," Prog. Quantum Electron. **28**(2), 113–143 (2004).
2. J. A. Piper and H. M. Pask, "Crystalline Raman lasers," IEEE J. Sel. Top. Quantum Electron. **13**(3), 692–704 (2007).
3. J. H. Lock and K. C. S. Fong, "Retinal Laser Photocoagulation," Med. J. Malaysia **65**(1), 88–94, quiz 95 (2010).
4. H. M. Pask, P. Dekker, R. P. Mildren, D. J. Spence, and J. A. Piper, "Wavelength-versatile visible and UV sources based on crystalline Raman lasers," Prog. Quantum Electron. **32**(3-4), 121–158 (2008).
5. A. S. Grabtchikov, V. A. Lisinetskii, V. A. Orlovich, M. Schmitt, R. Maksimenka, and W. Kiefer, "Multimode pumped continuous-wave solid-state Raman laser," Opt. Lett. **29**(21), 2524–2526 (2004).
6. A. A. Demidovich, A. S. Grabtchikov, V. A. Lisinetskii, V. N. Burakevich, V. A. Orlovich, and W. Kiefer, "Continuous-wave Raman generation in a diode-pumped Nd^{3+}:KGd(WO$_4$)$_2$ laser," Opt. Lett. **30**(13), 1701–1703 (2005).
7. H. M. Pask, "Continuous-wave, all-solid-state, intracavity Raman laser," Opt. Lett. **30**(18), 2454–2456 (2005).
8. Y. Lü, X. Zhang, S. Li, J. Xia, W. Cheng, and Z. Xiong, "All-solid-state cw sodium D$_2$ resonance radiation based on intracavity frequency-doubled self-Raman laser operation in double-end diffusion-bonded Nd^{3+}:LuVO$_4$ crystal," Opt. Lett. **35**(17), 2964–2966 (2010).
9. W. Lubeigt, V. G. Savitski, G. M. Bonner, S. L. Geoghegan, I. Friel, J. E. Hastie, M. D. Dawson, D. Burns, and A. J. Kemp, "1.6 W continuous-wave Raman laser using low-loss synthetic diamond," Opt. Express **19**(7), 6938–6944 (2011).
10. J. Jakutis-Neto, J. Lin, N. U. Wetter, and H. Pask, "Continuous-wave watt-level Nd:YLF/KGW Raman laser operating at near-IR, yellow and lime-green wavelengths," Opt. Express **20**(9), 9841–9850 (2012).
11. O. Kitzler, A. McKay, and R. P. Mildren, "Continuous-wave wavelength conversion for high-power applications using an external cavity diamond Raman laser," Opt. Lett. **37**(14), 2790–2792 (2012).
12. P. Dekker, H. M. Pask, D. J. Spence, and J. A. Piper, "Continuous-wave, intracavity doubled, self-Raman laser operation in Nd:GdVO$_4$ at 586.5 nm," Opt. Express **15**(11), 7038–7046 (2007).
13. A. J. Lee, H. M. Pask, D. J. Spence, and J. A. Piper, "Efficient 5.3 W cw laser at 559 nm by intracavity frequency summation of fundamental and first-Stokes wavelengths in a self-Raman Nd:GdVO$_4$ laser," Opt. Lett. **35**(5), 682–684 (2010).
14. T. Omatsu, M. Okida, A. Lee, and H. M. Pask, "Thermal lensing in a diode-end-pumped continuous-wave self-Raman Nd-doped GdVO$_4$ laser," Appl. Phys. B **108**(1), 73–79 (2012).
15. A. A. Kaminskii, K. Ueda, H. J. Eichler, Y. Kuwano, H. Kouta, S. N. Bagaev, T. H. Chyba, J. C. Barnes, G. M. A. Gad, T. Murai, and J. Lu, "Tetragonal vanadates YVO$_4$ and GdVO$_4$ – new efficient χ$^{(3)}$ - materials for Raman lasers," Opt. Commun. **194**(1-3), 201–206 (2001).
16. Y. F. Chen, "Compact efficient self-frequency Raman conversion in diode-pumped passively Q-switched Nd:GdVO$_4$ laser," Appl. Phys. B **78**(6), 685–687 (2004).
17. Y. F. Chen, "High-power diode-pumped actively Q-switched Nd:YVO$_4$ self-Raman laser: influence of dopant concentration," Opt. Lett. **29**(16), 1915–1917 (2004).

18. H. Zhu, Y. Duan, G. Zhang, C. Huang, Y. Wei, W. Chen, Y. Huang, and N. Ye, "Yellow-light generation of 5.7 W by intracavity doubling self-Raman laser of YVO$_4$/Nd:YVO$_4$ composite," Opt. Lett. **34**(18), 2763–2765 (2009).
19. F. Shuzhen, Z. Xingyu, W. Qingpu, L. Zhaojun, L. Lei, C. Zhenhua, C. Xiaohan, and Z. Xiaolei, "1097nm Nd:YVO$_4$ self-Raman laser," Opt. Commun. **284**(6), 1642–1644 (2011).
20. P. Dekker, H. M. Pask, and J. A. Piper, "All-solid-state 704 mW continuous-wave yellow source based on an intracavity, frequency-doubled crystalline Raman laser," Opt. Lett. **32**(9), 1114–1116 (2007).
21. F. Su, X. Zhang, Q. Wang, S. Ding, P. Jia, S. Li, S. Fan, C. Zhang, and B. Liu, "Diode pumped actively Q-switched Nd:YVO$_4$ self-Raman laser," J. Phys. D Appl. Phys. **39**(10), 2090–2093 (2006).
22. S. Ding, M. Wang, S. Wang, and W. Zhang, "Investigation on LD end-pumped passively Q-switched c-cut Nd: YVO$_4$ self-Raman laser," Opt. Express **21**(11), 13052–13061 (2013).
23. X. Li, A. J. Lee, H. M. Pask, J. A. Piper, and Y. Huo, "330 mW CW yellow emission from miniature self-Raman laser based on direct HR-coated Nd:YVO$_4$ crystal," IQEC/CLEO Pacific Rim, p. C289 (2011).
24. J. Lin and H. M. Pask, "Cascaded self-Raman lasers based on 382 cm^{-1} shift in Nd:GdVO$_4$," Opt. Express **20**(14), 15180–15185 (2012).
25. E. Rittweger, K. Y. Han, S. E. Irvine, C. Eggeling, and S. W. Hell, "STED microscopy reveals crystal colour centres with nanometric resolution," Nat. Photonics **3**(3), 144–147 (2009).
26. T. C. Damen, S. P. S. Porto, and B. Tell, "Raman Effect in Zinc Oxide," Phys. Rev. **142**(2), 570–574 (1966).
27. J. T. Murray, W. L. Austin, and R. C. Powell, "Intracavity Raman conversion and Raman beam cleanup," Opt. Mater. **11**, 353–371 (1999).
28. G. M. Bonner, Institute of Photonics, University of Strathclyde, 106 Rottenrow East, Glasgow, G4 0NW, UK, (personal communication, 2013).
29. X. Li, A. J. Lee, Y. Huo, H. Zhang, J. Wang, J. A. Piper, H. M. Pask, and D. J. Spence, "Managing SRS competition in a miniature visible Nd:YVO$_4$/BaWO$_4$ Raman laser," Opt. Express **20**(17), 19305–19312 (2012).

1. Introduction

Stimulated Raman Scattering (SRS) can be used to extend the wavelength coverage of common crystalline laser gain media [1,2]. This extended coverage benefits many applications especially when SRS is used in conjunction with Second Harmonic Generation (SHG) or Sum Frequency Generation (SFG) impacting medicine (retinal laser photocoagulation) [3], laser projection displays, and remote sensing (bathymetry or underwater detection) [4]. All-solid-state continuous-wave (CW) Raman lasers are widely recognized as a practical and efficient way to produce laser outputs in the near infrared, visible and ultraviolet wavebands [5–11]. Typically, intracavity Raman lasers feature a separate Raman active crystal inserted inside a laser resonator. However, simpler cavity design and reduced optical losses can be achieved using a self-Raman configuration whereby the laser gain medium is also used as Raman gain medium [12,13]. However, this configuration amplifies the thermal lensing inherent to SRS and laser conversion and also facilitates the onset of excited-state absorption or impurity absorption [12,14]. Over the last decade, Neodymium-doped Ortho-Vanadates, such as Nd:YVO$_4$ and Nd:GdVO$_4$ have been widely used in intracavity self-Raman lasers due to their good thermal properties and high Raman gain coefficient of 4.5cm/GW for their strongest Raman shift [13,15–23]. Only recently, several groups have used such materials to produce a more-closely spaced set of wavelength outputs between 1064nm and 1180nm based on a shorter secondary Raman shift. In 2011, Shuzhen et al. reported a pulsed c-cut Nd:YVO$_4$ self-Raman laser emitting at λ = 1097nm utilizing a 259cm^{-1} secondary Raman transition [19]. In 2012, Lin et al. demonstrated a-cut, self-Raman Nd:GdVO$_4$ lasers operating in the quasi-CW regime with 50% duty cycle and emitting at λ = 1108nm, 1156nm and 1227nm using the 882cm^{-1} and 382cm^{-1} Raman shifts [24]. True CW operation could not be achieved in this work because of strong thermal lensing in the Nd:GdVO$_4$ crystal [24].

In this paper, we report for the first time to our knowledge a Nd:YVO$_4$ self-Raman laser designed for secondary Raman shift (379cm^{-1}) and operating at the CW regime. To reduce the impact of the thermal lensing inherent to SRS, a miniature (26mm long) two-mirror cavity was designed using a strongly-concave output coupler (radius of curvature (ROC) = 0.1m) and a flat end-mirror. In this way, the thermal lens effect building up within the Nd:YVO$_4$ crystal inherent to SRS and laser conversion had a reduced effect on the cavity

dynamics and particularly the resonator stability. Therefore, true CW operation from the secondary Raman shift could be achieved. Three CW lasers emitting at λ = 1109nm, 1158nm and 1231nm were demonstrated. These wavelengths represent a significant addition to the more traditional self-Raman Nd:YVO$_4$ laser emitting at λ = 1176nm and using the primary Raman shift. In addition, these closely-spaced wavelengths can be utilised in conjunction with SHG or SFG to produce an even more-closely spaced set of visible lines in the green-lime-yellow region for biophotonic applications and in particular STED microscopy [25].

Several two-mirror laser resonators were developed. In each configuration, a particular wavelength output was favored by using an appropriate output coupler corresponding to the chosen Raman shift of Nd:YVO$_4$. In case 1, we demonstrated the oscillation of the first Stokes output at λ = 1109nm using the 379cm^{-1} Raman shift. In case 2, the second Stokes output of the 379cm^{-1} Raman shift emitting at λ = 1158nm was observed. In case 3, the combination of the 379cm^{-1} secondary Raman shift and the 893cm^{-1} primary Raman shift led to laser oscillation at λ = 1231nm.

In section 2, the measurement of the Raman spectrum for the a-cut Nd:YVO$_4$ crystal used in this work will be presented. Section 3 describes the experimental laser configurations. In section 4, the performance of several CW self-Raman lasers will be presented while a discussion will be provided in section 5.

2. Spontaneous Raman spectrum for the Nd:YVO$_4$ crystal

The spontaneous Raman spectrum for the a-cut, 20-mm long, 2mm diameter, 0.3 at. % doped Nd:YVO$_4$ crystal used in this paper was measured using a RENISHAW INVIA Raman microscope (see Fig. 1(a)). The microscope operated in a back scattering mode with 2cm^{-1} data resolution and used a λ = 514nm Argon laser as excitation. The laser beam propagated along one a-axis and was polarised along the c-axis of the Nd:YVO$_4$ crystal while the backscattered Raman signal component was also polarised along the c-axis. This scattering configuration can then be presented as X(ZZ)according to the Porto notations [26]. In Fig. 1(a), three main Raman shifts at 893cm^{-1}, 840cm^{-1} and 379cm^{-1} can be observed. The slight deviation from the Raman spectrum observed in [15] can be explained by minor variations in the manufacturing process. The strongest 893cm^{-1} Raman shift has been widely used in self-Raman lasers and corresponds to a λ = 1176nm wavelength output. Based on the Raman gain for 893cm^{-1} measured at 4.5cm/GW [15], the Raman gain for 379cm^{-1} can be estimated to be 0.9cm/GW using the relative ratio observed in Fig. 1(a). In addition, the full width at half maximum (FWHM) of the 893cm^{-1}, 840cm^{-1} and 379cm^{-1} shifts were measured at 6cm^{-1}, 6cm^{-1} and 14cm^{-1} respectively.
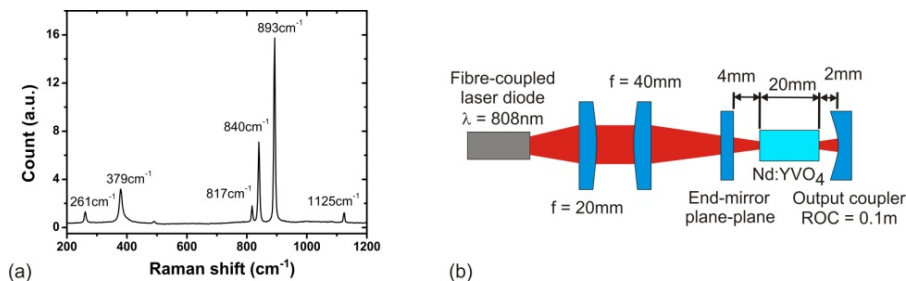

Fig. 1. (a) Raman spectrum of the a-cut Nd:YVO$_4$ rod with X(ZZ)scattering configuration and (b) schematic diagram of the self-Raman Nd:YVO$_4$ laser configuration.

3. Experimental configuration

The three lasers reported in this paper used the 2-mirror, 26mm-long cavity, shown in Fig. 1(b), albeit with different output couplers. A fibre-coupled laser diode (core diameter = 100μm, NA~0.22) capable of producing up to 30W at λ = 808nm was used as pump source.

Two plano-convex lenses focused the pump beam resulting in a 100μm beam waist at the middle of the gain medium. The Nd:YVO₄ rod characterised in section 2, was wrapped with indium foil and mounted in a water-cooled copper block so that the c-axis of the crystal corresponds to the horizontal axis (x-axis). Both side surfaces of the crystal were anti-reflection (AR) coated at λ = 1064, 1109-1176nm (reflectivity (R) <0.1%) and λ = 808nm (R<8%). Approximately, 96% of the total pump light was absorbed within the gain medium. The flat end-mirror was high-reflectivity (HR) coated (R>99.95% @ λ = 1064 & 1109-1230nm) and all concave (ROC = 0.1m) output couplers had a reflectivity above 99.97% at λ = 1064nm. An extracavity prism was used to separate the different output beams.

For case 1 investigating the laser emitting at λ = 1109nm, an output coupler with a transmission (T) of 0.2% and T>7% at λ = 1109nm and λ = 1158-1176nm respectively was used to favor the first Stokes output of the 379cm⁻¹ Raman shift. In case 2, an output coupler with T = 1.2%, 0.1% and 5.0% at λ = 1158nm, 1109nm, and 1176nm respectively was utilized to obtain the second Stokes output of the 379cm⁻¹ shift (λ = 1158nm). Finally, in case 3, an output coupler with T = 2.4%, 0.5%, 0.1% and 2.5% at λ = 1231nm, 1158nm, 1109nm and 1176nm respectively was used to achieve a laser output at λ = 1231nm which corresponds to the fundamental field being first converted to λ = 1109nm using the 379cm⁻¹ Raman shift and subsequently converted using the 893cm⁻¹ shift.

4. Results

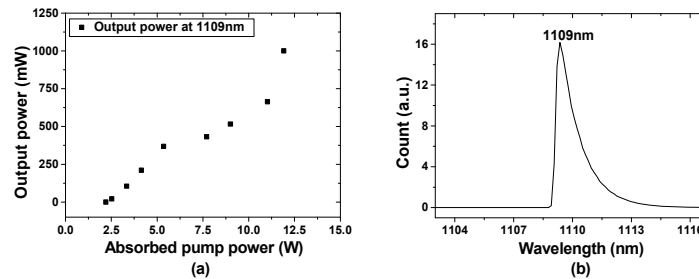*4.1 Case 1: Laser operating at λ = 1109nm based on the first Stokes output of the 379cm⁻¹ shift*

Fig. 2. (a) Power transfer of the λ = 1109nm output power and (b) optical spectrum of the Raman laser output at maximum output power for λ = 1109nm.

The optical power transfer at λ = 1109nm is shown in Fig. 2(a). Threshold for SRS was achieved at an absorbed laser diode pump power of 2.2W. A maximum output power of 1.0W was obtained for an absorbed laser diode pump power of 11.9W and fundamental output power of 70mW. This corresponds to an absorbed pump power to Raman output power conversion efficiency of 8.4%. The beam quality M² factors along the x and y transverse axes were measured at 2.3 and 3.1 for the λ = 1109nm laser output and 4.9 and 5.4 for the fundamental laser beam. Using an optical spectrum analyser (Agilent 86140B), the optical spectrum was measured and is displayed in Fig. 2(b). The FWHM linewidth of the first Stokes output can be estimated at 1.0nm with a resolution of 0.2 nm.

4.2 Case 2: Laser emitting at λ = 1158nm based on the 2nd Stokes output of the 379cm⁻¹ shift

The optical power transfer of the λ = 1158nm laser is shown in Fig. 3(a). In this case, the threshold for SRS at the second Stokes output was reached for an absorbed laser diode pump power of 8.6W. At this level, a first Stokes output power of 185mW and fundamental output power of 100mW could also be detected. The maximum output power obtained at λ = 1158nm was measured at 700mW for an absorbed laser diode pump power of 12.9W. This corresponds to an absorbed pump power to Raman output power conversion efficiency of

5.4%. At this pump level, first Stokes and fundamental output powers of 200mW and 150mW could also be observed respectively. The beam quality M^2 factors along the transverse x and y axes were both 1.2 for the $\lambda = 1158$nm beam, 1.8 and 1.9 for the $\lambda = 1109$nm beam and 3.4 and 3.6 for the fundamental laser. The spectrum of the Raman laser outputs is shown in Fig. 3(b).
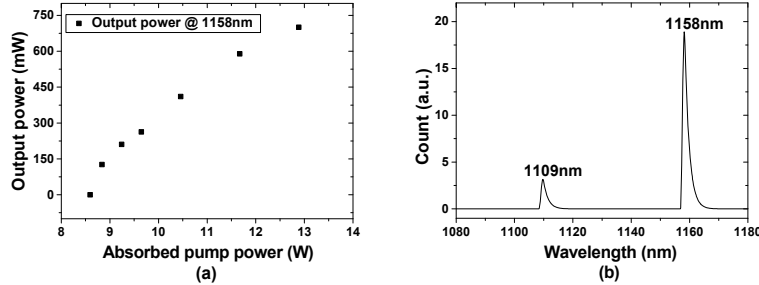

Fig. 3. (a) Power transfer of the $\lambda = 1158$nm output power and (b) optical spectrum of the Raman laser outputs at maximum output power for $\lambda = 1158$nm (resolution bandwidth: 1nm).

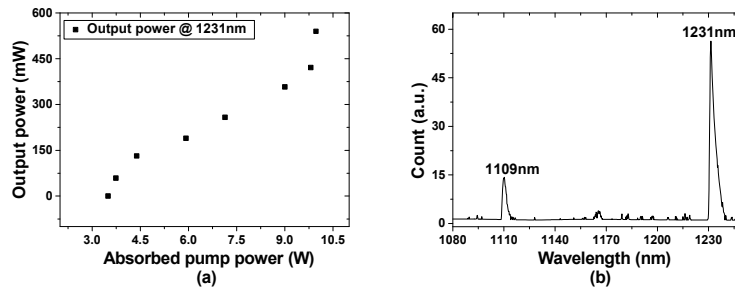*4.3 Case 3: Laser operating at 1231nm combining the 379cm^{-1} shift with the 893cm^{-1} shift*

Fig. 4. (a) Power transfer of the $\lambda = 1231$nm output power and (b) optical spectrum of the Raman laser outputs at maximum output power for $\lambda = 1231$nm (resolution bandwidth: 1nm).

The power transfer of the Raman laser operating at $\lambda = 1231$nm is shown in Fig. 4(a). The high transmission (T = 2.5%) at $\lambda = 1176$nm combined with low transmission at $\lambda = 1109$nm (T = 0.1%) of the output coupler meant that the Raman threshold for the $\lambda = 1109$nm oscillation was reached first. Therefore this Raman shift conversion acted as a loss mechanism for the fundamental signal preventing any oscillation of the 1176nm signal. In this way, the fundamental laser was first converted using the 379cm^{-1} shift before experiencing the 893cm^{-1} shift. The threshold for oscillation at this wavelength was reached for an absorbed laser diode pump power of 3.5W. At this pump level, first Stokes output power ($\lambda = 1109$nm) of 181mW and fundamental output power of 68mW were also recorded. A maximum output power of 540mW at $\lambda = 1231$nm was obtained for an absorbed laser diode pump power of 10W with the presence of first Stokes output power of 350mW and fundamental output power of 120mW. The absorbed pump power to Raman output power at $\lambda = 1231$nm conversion efficiency was then 5.4%. The beam quality M^2 factors along the x and y transverse axes were measured at 1.2 and 1.3 for the $\lambda = 1231$nm laser, 1.8 and 2.3 for the $\lambda = 1109$nm laser and 4 and 3.8 for the fundamental laser. The spectrum of the Raman lasers is shown in Fig. 4(b).

5. Discussion

The Raman beam clean-up effect [27] could be observed in all cases leading to a significant beam quality improvement of the Raman lasers compared to that of the fundamental output.

In order to put our results into context, the two-mirror cavity was designed to optimise CW operation at $\lambda = 1176$nm (i.e. the first Stokes of the strongest Raman shift). Therefore, a T = 1.0% output coupler at $\lambda = 1176$nm (with T<0.4% at 1109-1158nm) was used. Raman oscillation was obtained with an absorbed diode pump power of 2.1W. Only the $\lambda = 1176$nm output could be observed with up to 1.14W of output power obtained with an absorbed laser diode pump power of 12.2W leading to an absorbed pump power to Raman output power conversion efficiency of 9.3%. The performance of this laser is similar to that of the Raman laser emitting at $\lambda = 1109$nm. Although the difference in output coupling between these two laser configurations may contribute to explain such a similarity in performance, we believe that the ~5 fold reduction in Raman gain did not produce a difference in laser performance as significant as one would imagine. This can be explained by two reasons. First, the reduced quantum defect experienced in case 1 will reduce thermal lensing in the gain medium. Second, the larger linewidth of the secondary Raman shift compared to that of the primary shift has the potential to improve the Raman conversion by discouraging any side-stepping of the wavelength of the fundamental laser mode [28,29] as observed in [12] where another spectral line of the fundamental signal appeared to avoid any SRS-induced loss. The larger linewidth of the 379cm^{-1} Raman shift has the potential to also convert this secondary fundamental laser line and therefore prevent this behaviour. In this way, SRS conversion will be enhanced compensating the decrease in Raman gain. Therefore, self-Raman lasers based on the secondary Raman shift can have conversion efficiencies comparable to that of self-Raman lasers based on the primary shift despite the significant reduction in Raman gain. This effect will be the subject of further investigation.

The performances of the lasers described in this paper were limited by several influencing factors. First, the use of an output coupler with a strongly-concave curvature required for CW oscillation has the effect of significantly reducing the beam radius of the fundamental transverse mode within the gain medium (~100μm). The high intracavity laser powers common to self-Raman lasers can damage the AR coatings of the Nd:YVO$_4$ surfaces. Therefore, when designing the laser cavity, a balance must be struck between the avoidance of coating damage and the need of maintaining a good resilience to thermal lensing. In addition, SRS will produce a thermal lens that will ultimately limit the maximum output powers. For this reason, the absorbed laser diode pump powers of our lasers was limited to ~13W. This corresponded to a maximum thermal lensing (resulting from SRS and laser conversion) which was estimated to f = 20mm using an ABCD-matrix-based software and the laser dynamics experimentally observed. Moreover, during the SRS process, a strong blue fluorescence from the crystal was observed. This light could be explained by excited-state absorption or impurity absorption which can also limit the performance of the Raman output [12,14]. Finally, the Raman laser performances could be enhanced by optimising the reflectivity of the output couplers.

6. Conclusion

To our knowledge, the first CW self-Raman Nd:YVO$_4$ lasers designed for secondary Raman transition (379cm^{-1}) are reported. In this work, the lower Raman gain of this shift, measured to be ~5-times lower than that at 893cm^{-1}, did not appear to significantly attenuate the performance of the Raman laser at $\lambda = 1109$nm. Three resonators have been presented and characterised producing up to 1.0W, 700mW and 540mW at $\lambda = 1109$nm, 1158nm and 1231nm respectively. These lasers represent a first step towards the develoment of CW, narrowly-spaced, visible lines in the green-lime-yellow region.

Acknowledgments